High order modulation format identification based on compressed sensing in optical fiber communication system

Bingxiang Hui (惠柄翔)[1], Xianfeng Tang (唐先锋)[1], Na Gao (高 娜)[1], Wenbo Zhang (张文博)[2], and Xiaoguang Zhang (张晓光)[1,*]

[1]*State Key Laboratory of Information Photonics and Optical Communications, Beijing University of Posts and Telecommunications, Beijing 100876, China*

[2]*School of Science, Beijing University of Posts and Telecommunications, Beijing 100876, China*

**Corresponding author: xgzhang@bupt.edu.cn*

Received May 27, 2016; accepted September 9, 2016; posted online October 21, 2016

We propose a method of modulation format identification based on compressed sensing using a high-order cyclic cumulant combined with a binary tree classifier. Through computing the fourth-order cyclic cumulant of the pretreated band signal, which is obtained by compressed sensing with the sampling rate much less than the Nyquist sampling value, the feature vector for classification is extracted. Simulations are carried out in the optical coherent fiber communication system with different modulation formats of multiple phase-shift keying and multiple quadrature amplitude modulation. The results indicate that this method can identify these modulation formats correctly and efficiently. Meanwhile, the proposed method is insensitive to laser phase noise and signal noise.

OCIS codes: 060.1660, 060.2330, 060.4510.
doi: 10.3788/COL201614.110602.

Current optical network architecture faces severe challenges resulting from the ever-increasing demand on bandwidth and network capacity. In order to increase the spectral efficiency of the optical channel, several advanced high-order modulation formats (multiple phase-shift keying (M-PSK) and multiple quadrature amplitude modulation (M-QAM)) are introduced into an optical network. In addition, optical networks are becoming more flexible and software defined[1,2]. Multiple modulation formats (MFI) are used in the fully programmable bandwidth variable transponders to achieve the required data rate over the transmission distance[3]. Hence, modulation format identification is important for the management of networking at the nodes to allocate network resources effectively[4]. Meanwhile, it is also important to identify the modulation format before applying the proper digital signal processing (DSP) algorithm to achieve the optimum performance for the received optical signal[5]. So MFI is one of the critical technologies in the software-defined network (SDN).

Exploration of MFI techniques in optical communication has just begun. Four different methods have been employed for optical MFI: a) identification from constellation diagrams using k-means, which requires carrier and phase recovery before MFI[6]; b) principal-component-analysis-based pattern recognition on asynchronous delay-tap plots, which can realize channel estimation in the meantime but needs large amounts of sampling points[7]; c) artificial-neural-networks-based identification, which needs prior training[8]; d) Stokes space and machine learning technique[9,10].

In this Letter, we propose a method of MFI based on compressed sensing (CS) combined with a high-order cyclic cumulant and a binary tree classifier, which is robust against all the previous drawbacks. CS is a signal processing technique for efficiently acquiring and reconstructing a signal. The sparsity of a signal can be exploited to recover it from far fewer samples than required by the Shannon–Nyquist sampling theorem. The different modulation format signals have different high-order comulants so that we can use the high-order cumulant to identify the modulation formats. This method does not need to perfect reconstruction for the compressed cycle spectrum, however it makes full use of the block sparse feature of a signal in the cyclic frequency section so that the required number of compressed measurements is greatly reduced. Numerical simulations are carried out to investigate the effectiveness of the proposed technique under different optical signal-to-noise ratios (OSNRs). OSNRs in the range of 10–30 dB and under a laser linewidth of 100 MHz (laser linewidth corresponds to the laser phase noise). Results indicate that identification of modulation formats is successfully realized with estimation accuracies in excess of 99%. They also have shown that the proposed technique is robust against intensity and phase noises in the system.

The system architecture used in our simulations is shown in Fig. 1. Simulations using VPI photonic simulation software (from VPI photoncis Cor.) and MATLAB are carried out to verify the above method. It consists of a transmitter that is able to generate five different modulation formats (28 GBaud BPSK, QPSK, 8PSK, 16QAM, and 32QAM), an additive white Gaussian noise channel to introduce the

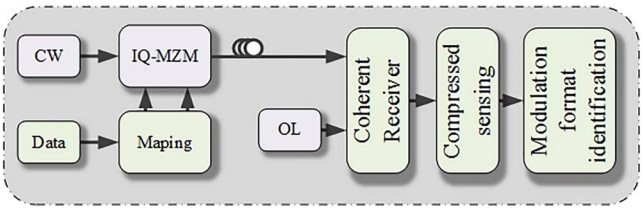

Fig. 1. System architecture of the simulated optical communications system.

variable power of noise, and a universal CS receiver capable of receiving any transmitted signals of the modulation formats.

The theory of CS as introduced by Candes, Romberg, and Tao and Domoho demonstrates that it has begun to be universally applied in signal reconstruction, medical imaging, radar, remote sensing, and other fields[11–16].

Suppose transmission signal $x \in R^N$ is an arbitrary K-sparse signal, $K \ll N$. The sparse reconstruction problem of CS is to estimate the sparse signal from the observed vector of measurements $y \in R^M$. The classical mathematical expression of the CS measurement equation is

$$y = \Phi x + z, \tag{1}$$

where $\Phi \in R^{M\times N}$ is a known measurement matrix with $M \ll N$ giving us information about x, and z denotes the measurement noise and model error. It is noted that the measurement matrix Φ needs to satisfy the restricted isometry property (RIP)

$$(1-\delta_K)\|x\|^2 \le \|\Phi x\| \le (1+\delta_K)\|x\|^2, \tag{2}$$

where δ_K is a restricted isometric constant. We will loosely say that a matrix Φ obeys the RIP of order K if δ_K is not too close to one. When this property holds, Φ approximately preserves the Euclidean length of K-sparse signals, which in turn implies that K-sparse vectors cannot be in the null space of Φ. An equivalent description of the RIP is to say that all subsets of K columns taken from Φ are in fact nearly orthogonal. This is useful as otherwise there would be no hope of reconstructing signal x. The next recognition is based on a higher-order cumulant that meets the sparse feature. We can take it as the target signal of the compression sampling signal.

Next, we analyze the kth-order cumulant of different single modulation formats, and analyze the possibility which is recognition parameters. The kth-order cumulant of a complex-valued stationary random process is

$$C_{k,x}(\tau_1,\tau_2,\ldots,\tau_{k-1}) = \mathrm{cum}(x(t), x(t+\tau_1), \ldots x(t+\tau_{k-1})), \tag{3}$$

where $x(t+\tau)$ denotes different delays of the same modulation signal, i.e.,

$$x(t), x(t+\tau_1), x(t+\tau_2), \ldots, x(t+\tau_{k-1}). \tag{4}$$

The fourth-order cumulant can be written as

$$\begin{aligned}\mathrm{cum}(x,y,z,w) = {} & E(xyzw) - E(xy)E(zw) \\ & - E(xz)E(yw) - E(xw)E(yz).\end{aligned} \tag{5}$$

The second- and fourth-order cyclic cumulants of the zero-mean $X(t)$, are shown as

$$C_{2,0}(\tau) = E\{x(t)x(t+\tau)\}, \tag{6}$$

$$\begin{aligned}C_{4,0}(\tau) = {} & E\{x(t)x(t+\tau_1)x(t+\tau_2)x(t+\tau_3)\} \\ & - C_{2,x}(\tau_1)C_{2,x}(\tau_2-\tau_3) - C_{2,x}(\tau_2)C_{2,x}(\tau_3-\tau_1) \\ & - C_{2,x}(\tau_3)C_{2,x}(\tau_1-\tau_2).\end{aligned} \tag{7}$$

In practice, the mean value of the sample signal is removed before the cumulant estimation. Sample estimating of the correlations are given by

$$C_{2,0} = E[x^2(t)] = \frac{1}{N}\sum_{n=1}^{N}(x(t))^2, \tag{8}$$

$$C_{2,1} = E(x(t)x^*(t+\tau)) = \frac{1}{N}\sum_{n=1}^{N}|x(t)|^2, \tag{9}$$

where the second- and fourth-order cumulants can be written as

$$\begin{aligned}C_{2,0} &= \mathrm{cum}(x(t)x(t)), \\ C_{2,1} &= \mathrm{cum}(x(t)x^*(t)), \\ C_{4,0} &= \mathrm{cum}(x(t)x(t)x(t)x(t)).\end{aligned} \tag{10}$$

Combining with Eqs. (3), (4), and (8), this leads to the following estimates:

$$C_{4,0} = \frac{1}{N}\sum_{n=1}^{N}|x(t)|^4 - 3C_{2,0}^2. \tag{11}$$

We can calculate the cumulants of the digital modulation signal, which are listed below in Table 1.

This recovery of the high-order cumulant method is based on the fact that most of the modulation signals have smooth circulation features and Gaussian white noise only emergent in the zero cyclic frequency. This introduces cyclic spectrum analysis into the compressive sensing framework and proposes the sparse signal detection

Table 1. kth-order Cumulant of Digital Modulation Signal

	BPSK	QPSK	8PSK	16QAM	32QAM
$C_{2,0}$	1	0	0.67	0	0
$C_{2,1}$	1	1	1	1	1
$C_{4,0}$	−2	1	0	−0.68	−0.19

methods in the basic compressed domain cyclic spectrum energy characteristics.

Because the high-order cumulant meets the sparse feature, we can make use of CS for its estimation,

$$[\![y]\!]^2 = \Phi[\![x]\!]^2, \tag{12}$$

where $[\![x]\!]^2 = |x(1)^2, x(2)^2, x(3)^2, ..., x(n)^2|$ and Φ is a known measurement matrix.

Given the received signal from Eq. (1), we get a frame of CS samples to simplify the reconstruction.

First, we derive a relationship between $R_{[\![y]\!]^2}$ and $R_{[\![x]\!]^2}$. R_{ξ} is a ξ vector sequence with an autocorrelation matrix sequence:

$$\begin{aligned} R_{[\![y_t]\!]^2} &= [\![y_t]\!]^2([\![y_t]\!]^2)^T = (\Phi[\![x_t]\!]^2)(\Phi[\![x_t]\!]^2)^T \\ &= \Phi R_{[\![x_t]\!]^2}\Phi^T. \end{aligned} \tag{13}$$

Second, we find a relationship between $[\![y]\!]^2$ and $R_{[\![y]\!]^2}$.

$$\mathrm{vec}(R_{[\![y_t]\!]^2}) = (\Phi \otimes \Phi)\mathrm{vec}(R_{[\![x_t]\!]^2}), \tag{14}$$

where the vec(·) operator creates a column vector from a matrix $\cdot = [a_1, a_2, ...a_n]$ by stacking its columns vertically: $\mathrm{vec}(\cdot) = [a_1, a_2, ...a_n]^T$.

(Important properties of the vec(·) operation are given below: $\mathrm{vec}(AXB) = (B^T \otimes A)\mathrm{vex}(X)$).

Using a result of Ref. [17], we can relate to $[\![y]\!]^2$ using mapping matrices.

$P_{[\![y]\!]^2} \in \{0,1\}^{N^2 \times \frac{N(N+1)}{2}}$ that map the entries in $[\![y]\!]^2$ with corresponding ones in $\mathrm{vec}(R_{[\![y_t]\!]^2})$:

$$[\![y_t]\!]^2 = P_{[\![y_t]\!]^2}\,\mathrm{vec}(R_{[\![y_t]\!]^2}). \tag{15}$$

Combining with Eqs. (11), (12), and (13),

$$[\![y_t]\!]^2 = P_{[\![y_t]\!]^2}\,\mathrm{vec}(R_{[\![y_t]\!]^2}) = P_{[\![y_t]\!]^2}(\Phi \otimes \Phi)\mathrm{vec}(R_{[\![x_t]\!]^2}). \tag{16}$$

Then, the fourth-order cyclic cumulant ($C_{4,0}$) can be estimated as

$$C^{\alpha}_{(4,0)} = F[\![x_t]\!]^4 - 3[\![F[\![x_t]\!]^2]\!]^2, \tag{17}$$

where $F = [\frac{1}{N}e^{-j2\pi\alpha n/N}]_{(\alpha,n)}$ is the n-point discrete Fourier transform (DFT) matrix.

In addition, $[\![x_t]\!]^4$ can be expressed as

$$\begin{aligned} [\![x_t]\!]^4 &= \mathrm{diag}(R_{[\![x_t]\!]^2}) = P_x\mathrm{vec}(R_{[\![x_t]\!]^2}) \\ &= P_x\mathrm{vec}([\![x_t]\!]^2([\![x_t]\!]^2)^T). \end{aligned} \tag{18}$$

Combining with Eqs. (17) and (18),

$$\begin{aligned} C_{4,0} &= FP_x\mathrm{vec}(R_{[\![x_t]\!]^2}) - 3P_{Fx}\mathrm{vec}(R_{F[\![x_t]\!]^2}) \\ &= FP_x\mathrm{vec}(R_{[\![x_t]\!]^2}) - 3P_{Fx}\mathrm{vec}(FR_{[\![x_t]\!]^2}F^T) \\ &= [FP_x - 2P_{Fx}(F \otimes F)]\mathrm{vec}(R_{[\![x_t]\!]^2}). \end{aligned} \tag{19}$$

Combining with Eqs. (16) and (19),

$$\begin{aligned} [\![y_t]\!]^2 &= P_{[\![y_t]\!]^2}(\Phi \otimes \Phi)\mathrm{vec}(R_{[\![x_t]\!]^2}) \\ &= P_{[\![y_t]\!]^2}(\Phi \otimes \Phi)[FP_x - 2P_{Fx}(F \otimes F)]^{\dagger}C_{4,0}. \end{aligned} \tag{20}$$

Equation (20) can be simplified as

$$\Gamma = \Theta C^{\alpha}_{(4,0)}, \tag{21}$$

where Θ and Γ can be written as

$$\begin{aligned} \Theta &= P_{[\![y_t]\!]^2}(\Phi \otimes \Phi)[FP_x - 2P_{Fx}(F \otimes F)]^{\dagger}, \\ \Gamma &= [\![y_t]\!]^2. \end{aligned}$$

The matrix Θ satisfies RIP rules. We can use the CS theory for $C_{4,0}$ estimation.

Finally, the system can use the CS sampling theory for MFI combined with the four-order cumulant and the binary tree classifier regardless of the actual noise variance. The decision rule used was

$$\begin{aligned} C_{4,0} &< 0.15 \Rightarrow \mathrm{8PSK}, \\ 0.15 \le C_{4,0} &< 0.34 \Rightarrow \mathrm{32QAM}, \\ 0.34 \le C_{4,0} &< 0.8 \Rightarrow \mathrm{16QAM}, \\ 0.8 \le C_{4,0} &< 1.4 \Rightarrow \mathrm{QPSK}, \\ 1.4 \le C_{4,0} &\Rightarrow \mathrm{BPSK}, \end{aligned} \tag{22}$$

with $C_{4,0}$ estimated as described in Equation (11).

Figure 2 shows the simulation setup. The dotted frame at the lower side of Fig. 2 shows the identification flow. It consists of a transmitter that is able to generate five different modulation formats (28 GBaud BPSK, QPSK, 8PSK, 16QAM, and 32QAM), laser linewidth and an additive white Gaussian noise channel introducing variable noise power, and a universal CS receiver capable of receiving any of the modulation formats transmitted. Through the simulation experiments, the theoretical analysis results are verified.

The recognition performance of the proposed methods are shown below in Figs. 3–5.

Figure 3 shows the fourth-order cyclic cumulant estimation versus OSNR under 50% Nyquist sampling factors.

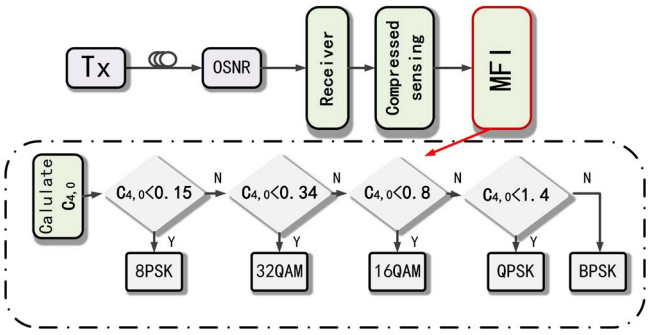

Fig. 2. Simulation setup and decision flowchart.

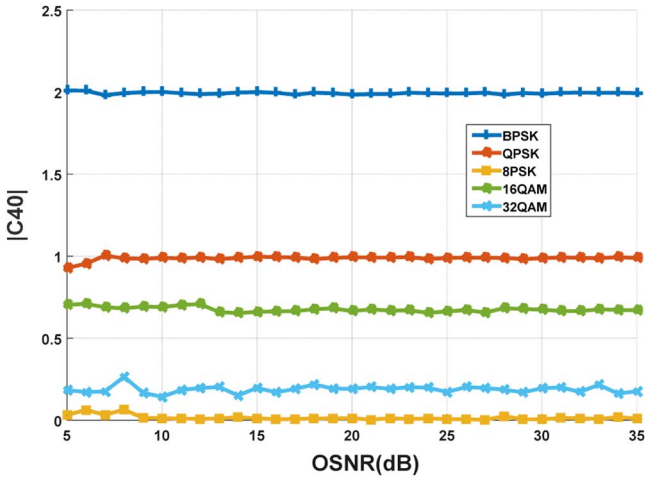

Fig. 3. 50% Nyquist sampling, 500 times the simulation $C_{4,0}$ mean recovery.

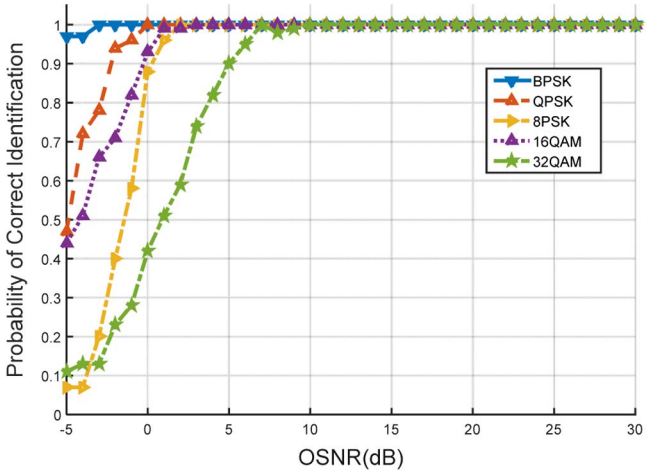

Fig. 4. Modulation format recognition success rate.

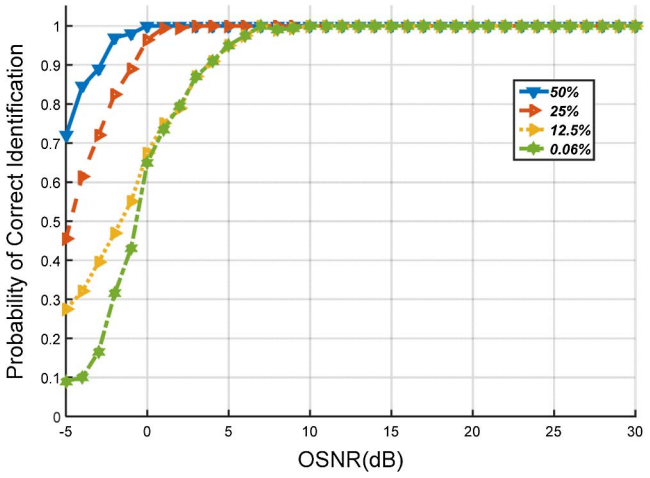

Fig. 5. Success rate under different compression ratios.

Figure 4 shows the modulation format recognition success rate versus OSNR under 50% Nyquist sampling factors. The results of the simulations demonstrate successful identification of modulation formats with estimation accuracies in excess of 99% under different OSNRs in the range of 10–30 dB. Figure 5 shows the success rate of identification versus OSNR under different compression ratio factors. We can see that the success rate of identification of the different modulation format signal e is more than 99% under different OSNRs in the range of 10–30 dB and under 0.06% of the Nyquist sampling rate.

We propose a method of MFI based on CS combined with a high-order cyclic cumulant and a binary tree classifier. In this work, our main contribution is to reconstruct the cyclic spectrum of a sparse signal directly from subNyquist-rate compressive samples without having to recover the signal itself. The simulation results indicate that this method can effectively realize signal detection for modulation format identification in low OSNR conditions. In addition, on the basis of the CS model, it gives an extraction method for the cyclic spectrum feature that is based on binary iteration and also combines it with a binary tree classifier for five kinds of common signal modulation recognition. This technique utilizes CS with a sampling rate much less than the Nyquist sampling rate and a binary tree classifier to enable low-cost identification at the receivers as well as at the intermediate network nodes without requiring any prior information from the transmitters.

This work was supported by the National Natural Science Foundation of China (Nos. 61571057 and 61501213), the Fund of State Key Laboratory of Information Photonics and Optical Communications (Beijing University of Posts and Telecommunications), P. R. China (No. IPOC2016ZT12), and the Open Fund of the Guangdong Provincial Key Laboratory of Optical Fiber Sensing and Communications (Jinan University)

References

1. H. Kim and N. Feamster, IEEE Commun. Mag. **51**, 114 (2013).
2. Y. Yu, Y. Zhao, J. Zhang, H. Li, Y. Ji, and W. Gu, Chin. Opt. Lett. **12**, 110602 (2014).
3. K. Roberts and C. Laperle, in *38th European Conference and Exhibition on Optical Communications (ECOC)* (Optical Society of America, 2012), Paper We.3.A.3.
4. A. Thyagaturu, A. Mercian, M. P. Mcgarry, M. Reisslein, and W. Kellerer, "Software defined optical networks (SDONs): A comprehensive survey," arXiv:1511.04376 (2015).
5. T. Bo, J. Tang, and C. C.-K. Chan, in *Optical Networking and Communication Conference & Exhibition (OFC)* (2016).
6. N. G. Gonzalez, D. Zibar, and I. T. Monroy, in *Proc. ECOC* (2010).
7. M. C. Tan, F. N. Khan, W. H. Al-Arashi, Y. D. Zhou, and A. P. T. Lau, J. Opt. Commun. Netw. **6**, 441 (2014).
8. F. N. Khan, Y. Zhou, A. P. Lau, and C. Lu, Opt. Express **20**, 12422 (2012).
9. R. Borkowski, D. Zibar, A. Caballero, V. Arlunno, and I. T. Monroy, IEEE Photon. Technol. Lett. **25**, 2129 (2013).

10. L. Cheng, L. Xi, D. Zhao, and X. Tang, Chin. Opt. Lett. **13**, 100604 (2015).
11. D. L. Donoho, IEEE Trans. Inf. Theory **52**, 1289 (2006).
12. E. Candès, in *Proceedings of International Congress of Mathematicians*, Madrid, Spain **3**, 1433 (2006).
13. E. J. Candès, J. Romberg, and T. Tao, IEEE Trans. Inf. Theory **52**, 489 (2013).
14. M. Sun, N. Feng, Y. Shen, J. Li, L. Ma, and Z. Wu, Chin. Opt. Lett. **9**, 061002 (2011).
15. M. Sha, J. Liu, X. Li, and Y. Wang, Chin. Opt. Lett. **12**, 060023 (2014).
16. E. J. Candes and T. Tao, IEEE Trans. Inf. Theory **52**, 5406 (2006).
17. Z. Tian, Y. Tafesse, and B. M. Sadler, IEEE J. Sel. Top. Signal Process. **6**, 58 (2012).